Tôhoku Geophys. Journ. (Sci. Rep. Tôhoku Univ., Ser. 5), Vol. 36, No. 2, pp. 47-63, 2001

Arctic Oscillation and Corresponding Sea Surface Temperature Anomaly Fields

SAYAKA YASUNAKA and KIMIO HANAWA

Department of Geophysics, Graduate School of Science,
Tohoku University Aoba-Ku, Sendai 980-8578

(Received October 31, 2000; accepted January 29, 2001)

Abstract: Empirical orthogonal function (EOF) and rotated EOF analyses of the monthly mean sea level pressure (SLP) anomalies reveal that the Arctic Oscillation (AO) activities include those of both the North Atlantic Oscillation (NAO) and the Polar-Eurasia pattern (POL).. However it is found that the NAO and the POL are not independent of each other.

Based on a regression analysis, it is also found that the organized sea surface temperature (SST) anomaly fields coherently varying with the AO exist in the North Atlantic and the North Pacific. EOF analysis is also applied to the monthly mean SST anomaly fields in the region north of 20°N. The mode closely relating to the AO appears as the second EOF mode. On the other hand, the first mode reveals a strong decadal fluctuation correlated with the activities of the Pacific/North American (PNA) pattern.

The AO index shows a significant jump in 1988/89. This climate jump appears clearly in the second SST-EOF mode (*i.e.*, AO) and partially in the first SST-EOF mode (*i.e.*, PNA). In contrast, the well-known climate jump occurring in 1976/77 is obseved only in the first SST-EOF mode.

1. Introduction

The term 'Arctic Oscillation' (AO) has recently been introduced by Thompson and Wallace (1998) to describe the dominant structure in sea level pressure (SLP) variabilities over the Northern Hemisphere. They showed that the leading mode (*i.e.*, AO) of an empirical orthogonal function (EOF) analysis for the Northern Hemisphere monthly mean SLP anomaly fields is a surface signature of coupled pattern of the Northern Hemisphere lower-stratospheric wintertime polar vortex fluctuations and a wave-like disturbance of geopotential height anomalies in the middle troposphere.

The AO resembles the well-known North Atlantic Oscillation (NAO) in many respects, but its primary region of action covers more wide area of the Arctic, giving it a more zonally symmetric appearance. In addition, the AO exists year-round in the troposphere, but it amplifies with height upward into the stratosphere during cold season in which the strength of a zonal flow is closely related with strong planetary wave-mean flow interaction in mid winter (Thompson and Wallace, 2000).

Kerr (1998) and Wallace (2000) pointed out that the AO and the NAO are different representations and conceptual interpretations of the same phenomenon. Other several investigations also argued that the AO is a preferred mode rather than the NAO, since the NAO index is not an optimal representation of the leading SLP structure of variabil-

ity in the Atlantic sector (Deser, 2000) and the AO representation is applicable to intraseasonal as well as interannual time scales, whereas the NAO is organized only in winter (Thompson *et al.*, 2000).

Overland *et al.* (1999) compared the AO with leading modes in 700 hPa geopotential height fields provided by Climate Prediction Center (CPC) at National Center for Environmental Prediction (NCEP). The first mode in December and February was named the Polar-Eurasia pattern (POL), which is very similar rather than the NAO to Thompson and Wallace (1998)'s 500 hPa geopotential height regression map on the AO, although activities of the POL are limited to three months of December, January and February.

Under the above mentioned controversy on the AO, the first purpose of the present study is to clarify a relationship between the AO and the NAO or the POL. Here, we will examine the SLP field using EOF and rotated EOF (REOF) analyses as well as a regression analysis.

On the other hand, in the ocean, an annular structure has not been clear. Since there are few data in the Arctic Ocean, it might be difficult to find a variability related with the polar vortex and the zonal ring of opposite sign. However, SST anomalies coherently varying in the North Atlantic and the North Pacific were shown by Kachi and Nitta (1997). They pointed out that this mode had a jump in the late-1980's and it is a different mode of the decadal mode with the well-known climate jump in the mid-1970's. In the late-1980's, SLP in the central Arctic and a sea ice over the Okhotsk Sea also decreased abruptly (Walsh *et al.*, 1996; Tachibana *et al.*, 1996).

Although Thompson *et al.* (2000) argued that the AO index exhibited a trend toward the high index polarity over a past few decades, this trend in the AO might be regarded as part of a fluctuation with much longer time scales as Wang and Ikeda (2000) speculated.

So, the second purpose is to investigate a relationship between the AO and SST anomaly fields, especially we focus a climate jump occurred in the late-1980's. Here, the similarity or difference of the late-1980's climate jump with that occurred in the mid-1970's is also examined.

The remainder of this paper is organized as follows. Data and analysis tools used in this study are outlined in Section 2. In Section 3, EOF and REOF analyses are applied to the monthly mean SLP anomaly fields to investigate a relationship between the AO and the NAO or the POL. Section 4 documents SST anomaly fields coherently varying with the AO by regression analysis and EOF analysis applied to monthly mean SST fields. We summarize the present study in Section 5.

2. Data and analysis tools

2.1. The data used

Various kinds of data are used in the present study : SLP, SST, 500 hPa geopotential height, sea surface wind (SSW) and activity indices of atmospheric teleconnection

patterns.

The monthly mean 5°×5° (lat.×lon.) SLP data are those prepared by Miyamoto (2000). The data period is from 1899 to 1998. These SLP data are based on those complied by Trenberth and Paolino (1980). Although this original data have many blank grids, Miyamoto and Hanawa filled those blank grids using the technique developed by Ward (1989) for generation of the Global Ice and Sea Surface Temperature (GISST) dataset. Readers may refer to Miyamoto (2000) on details of the data.

The monthly mean 5°×5° SST data are prepared by the authors. The data period is from 1854 to 1997. The individual SST reports archived in the Comprehensive Ocean-Atmosphere Data Set (COADS) and in the recently released Kobe Collection (Manabe, 1999) are used in computation. Although these data cover the global oceans, there are many blank grids especially in equatorial area and oceans in the Southern Hemisphere in space and in the early stages in time. The details of this newly prepared SST data will be described elsewhere by the authors.

The monthly mean 5°×5° 500 hPa geopotential height data are those from NCEP-National Center for Atmospheric Research (NCAR) reanalysis (Kalnay *et al.*, 1996). The data period is from 1948 to 1998.

The monthly mean 5°×5° SSW data were produced by Hanawa and Yasuda (2000). These SSW data were reconstructed using SLP field and cover the North Pacific north of 20°N for the period from 1899 to 1995. The details of this data can be referred to Hanawa and Yasuda (2000).

For each of these data, we compute climatological monthly mean values for 30 years from 1961 to 1990 at each grid point. Then, we define a monthly mean anomaly as a departure from climatological mean value. These anomaly fields are used in analyses.

The monthly teleconnection pattern indices such as the NAO, the POL and so on, are cited from the web site of CPC at NCEP (http://www.cpc.ncep.noaa.gov/data/teledoc/telecontents.html), which is based on the leading modes of variabilities in the 700 hPa geopotential height fields. These monthly indices are the standardized amplitudes constructed from REOF analysis for each month (Barnston and Levizey, 1987; Bell and Halpert, 1995).

The AO index is that defined by Thompson and Wallace (2000), using all months of the year, on the basis of the standardized time series of the leading EOF mode of monthly mean Northern Hemisphere SLP anomalies for the region north of 20°N.

2.2. Analysis tools

In the present study, conventional EOF and REOF analyses are employed. Both covariance matrix and correlation matrix methods are used for the monthly mean anomalies for 40 years from 1958 to 1997.

In these analyses, we pay our attention on the grid arrangement. In some case, the data are weighted by a square root of cosine of latitude. In another case, 'irregularly' arranged grids which have less numbers per longitude near the pole than at the lower latitude are used, in order to realize uniform grid spacing in a unit area. Actual grid

numbers are 72 on latitudinal circles from 20 to 55°N, 36 from 60 to 75°N, 18 at 80°N, and 9 at 85°N. No grid is given at the pole. However, since SST data are almost blank in the polar region, the above treatments are not adopted.

In REOF analysis, eigenvector frames of EOF modes are linearly transformed to minimize the extent of regions with strong correlation between the original data and the rotated EOF modes, *i.e.* to maximize the square of variance of factor loadings. Here, when the correlation matrix method is used in REOF calculation, factor loadings are equivalent to eigenvectors multiplied by the square roots of their eigenvalues. This method is called 'a varimax orthogonal rotation', which is widely accepted as the most accurate analytic algebraic orthogonal rotation (Richman, 1986). The REOF modes are generally gained at the expense of losing the uncorrelatedness of time coefficients. However, REOF analysis can extract two independent modes when they have similar spatial patterns (*c.f.* Preisendorfer, 1988).

Only the first 10 unrotated modes are used in rotation. These first ten modes include about 80% of the original variance. The loadings pattern of the first five EOFs remains identical if at least ten initial EOFs are rotated (Horel, 1981). For confirmation, when 20 modes are rotated instead of 10, the results are not different.

When we present the result of REOF analysis, distribution of factor loadings is displayed as well as time coefficient. Here, factor loadings can be regarded as correlation coefficient between time coefficient and time series at each grid point.

A regression analysis is also applied to investigate variabilities associated with various indices. When the results of EOF analyses are displayed, the regression analysis is used to show variabilities at all grid points including grid points not used in EOF calculation because of a lack of data. Since the time series are standardized to be dimensionless, these 'regression maps' have the same units as the anomaly fields themselves.

3. Variability of monthly mean SLP anomaly fields

In this section we apply EOF and REOF analyses to the monthly mean SLP anomaly fields to examine their variabilities and to clarify a relationship of the AO with the NAO or the POL.

3.1. Variability of monthly mean SLP anomaly fields in the Northern Hemisphere

As mentioned in Introduction, Thompson and Wallace (2000) showed the AO is the most dominant feature in the monthly mean SLP anomaly fields in the Northern Hemisphere. In order to confirm it in Miyamoto's SLP data, EOF analysis by a covariance matrix method is applied to the monthly mean SLP anomaly fields, which are weighted by a square root of cosine of latitude in the region north of 20°N (see Section 2.2). The data period treated is 40 years from 1958 to 1997 which is the same as that of Thompson and Wallace (2000).

Figure 1 shows the standardized time coefficient of the first EOF mode and SLP

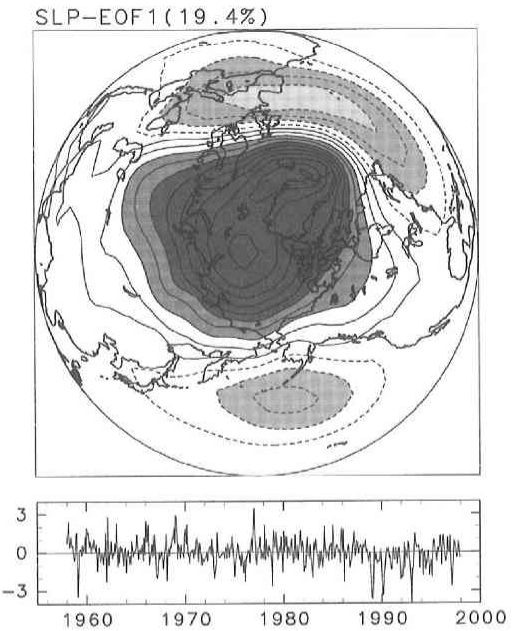

Fig. 1. SLP anomalies regressed upon the standardized time coefficient (upper panel) and the standardized time coefficient of the first SLP-EOF mode extracted by a covariance matrix method for the region north of 20°N from 1958 to 1997 (lower). Anomalies of all months through the year are used in calculation. Contour interval is 1 hPa. Negative contours are dashed.

anomaly field regressed upon the standardized time coefficient. This mode can account for 19.4% of the total variance. The regression map is characterized by a maximum at the polar region surrounded by a zonal ring of opposite sign, and it is largely zonally symmetric. These features are identical to that derived from the analysis of Thompson and Wallace (2000). In addition, correlation coefficient between the time coefficient obtained here and the AO index defined by Thompson and Wallace (2000) exceeds −0.99. Here, note that this negative correlation coefficient comes from the reversed sign in time coefficient with that in Thompson and Wallace (2000). This result confirms that the most dominant mode is the AO, even in the monthly mean SLP anomaly fields used in this study. So, in the following analyses, we use the AO index defined by Thompson and Wallace (2000) as an indicator of AO activity, to make comparison with the previous studies easy.

3.2. Relationship between AO and NAO or POL

In this subsection, January and February SLP variabilities are focussed, since the NAO and the POL as well as the AO are dominant modes in these months (Barnston and Livezey, 1987 ; Thompson and Wallace, 1998).

Figure 2 shows the regression maps of SLP anomaly on the standardized NAO and POL indices in January. Although there is no correlation between the NAO index and

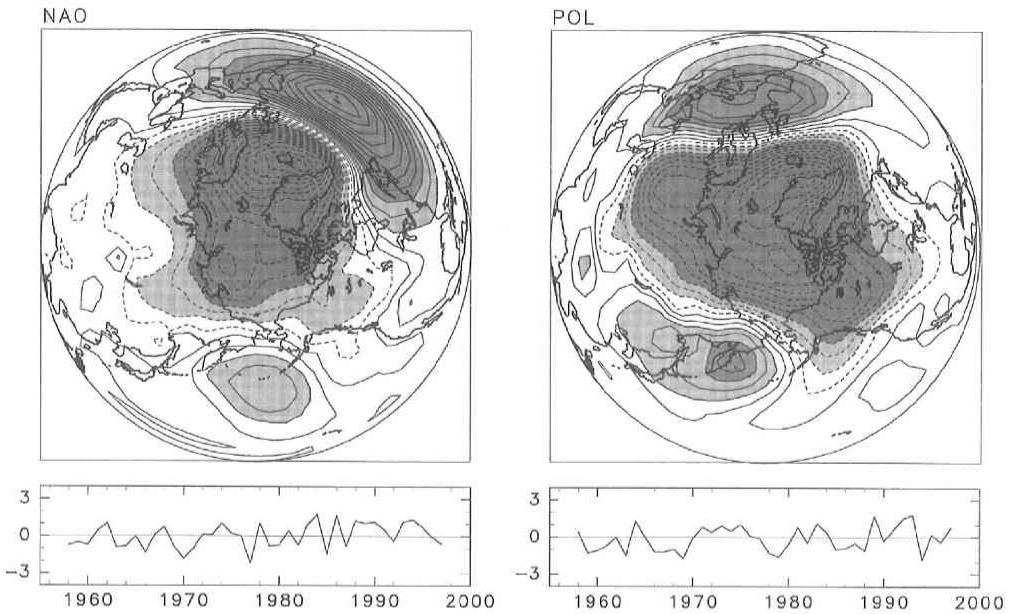

Fig. 2. SLP anomaly fields regressed upon the standardized NAO index (a) and POL index (b) in January. Contour interval is 1 hPa. Negative contours are dashed.

the POL index, these two maps are similar to each other. They have a large response in the polar region and the opposite response in the North Pacific and the North Atlantic. The NAO response in the North Atlantic is greater than that in the North Pacific, while the POL responses over both the basins have similar magnitude. The center of the POL response in the North Atlantic is situated east rather than that of the NAO. The regression maps of February shows almost the same feature as those of January.

Then, EOF and REOF analyses are applied to the monthly mean SLP anomaly fields for the region north of 20°N for each month, using irregularly arrannged grids. The analysis period is again 40 years from 1958 to 1997.

Figure 3 shows the distribution of factor loadings and time coefficient of the first EOF mode before rotation in January. This mode accounts for 22.6% of the total variance and is separated well from the other modes, since the second mode is account for only 12.5%. The distribution of factor loadings is very similar to Fig. 1 and therefore we can regard this mode as the AO. Actually, time coefficient of this mode is well correlated with the AO index (correlation coefficient $R=-0.93$).

Using the first ten EOF modes, REOF modes are extracted. Figure 4 shows the distributions of factor loadings and time coefficients of the two leading REOF modes in January. The distribution of factor loadings of the first (second) mode is very similar to the SLP anomaly fields regressed upon the NAO (POL) index as shown in Fig. 2. Actually, the correlation coefficient between time coefficient of the first (second) mode and the NAO (POL) index is 0.90 (−0.80). Therefore, we can say that the first REOF mode corresponds to the NAO and the second REOF mode to the POL. Since the first

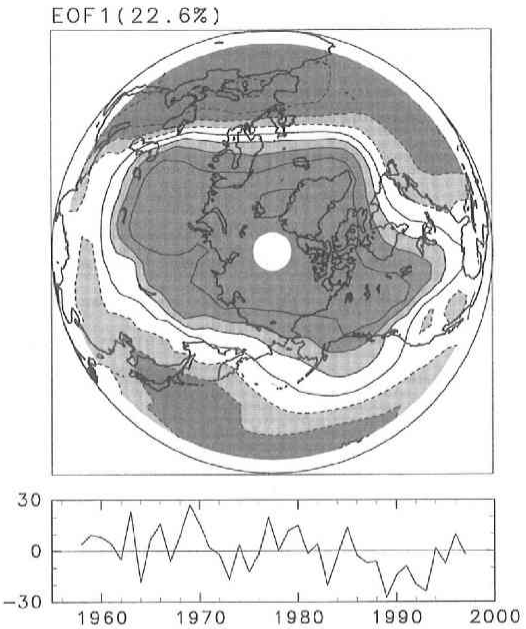

Fig. 3. Distribution of factor loadings (upper panel) and time coefficient (lower) of the first SLP-EOF mode in January, extracted by a correlation matrix method for the region north of 20°N from 1958 to 1997. Contour interval is 0.2. Negative contours are dashed.

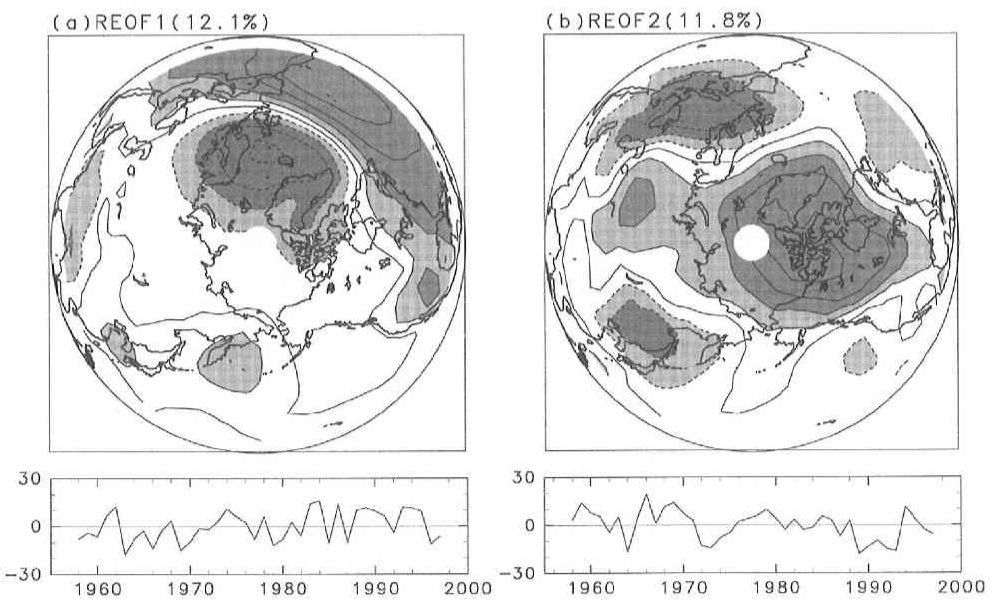

Fig. 4. Distributions of factor loadings (upper panel) and time coefficients (lower) of the first (a) and second (b) SLP-REOF modes in January, extracted by a correlation matrix method for the region north of 20°N from 1958 to 1997. Contour interval is 0.2. Negative contours are dashed.

EOF mode (AO) has a high correlation with the two REOF leading modes (NAO and POL), it can be said that both the NAO and the POL are derived from the AO. However the first and second REOF modes are not independent (although eigenvectors of the two modes are orthogonal by definition, time coefficients have correlation; $R=-0.35$). Actually regression maps on the NAO and POL indices (Fig. 2) are similar to each other as mentioned above. Therefore the SLP variabilities represented by the AO can not be separated into the NAO and the POL perfectly. In addition, it is found that the NAO and the POL in February are contaminated to some degree in the first REOF mode.

The above result clearly shows that the AO is the most leading and basic structure of variabilities in the Northern Hemisphere SLP anomaly fields, and includes variabilities represented by the NAO and the POL. As a result, we can regard the AO as a good indicator of SLP anomaly fields rather than the POL or the NAO itself.

4. SST anomaly fields coherently varying with AO

In this section we examine SST anomaly fields coherently varying with the AO. Although the AO exists year-round in the troposphere as mentioned before, we focus our attention only on winter season, since the active season of the AO is winter from January to March (Thompson and Wallace, 2000).

4.1. Regression analyses with AO

Regression analyses are performed to the monthly mean SST, SSW, 500 hPa geopotential height and SLP anomaly fields upon the AO index in winter. The result is shown in Fig. 5. As a matter of course, the regression map of the SLP anomalies (Fig. 5e) resembles very well Fig. 1 and that of 500 hPa geopotential height anomalies (Fig. 5d) shows almost the same pattern as that shown by Thompson and Wallace (1998). Both the regression maps show the stronger polar jet, Icelandic Low (IL) and Azores High (AH) and the weaker Aleutian Low (AL). The less zonally symmetric feature of the 500 hPa geopotential height field rather than that of the SLP field might be caused by contamination of a baroclinic signature (Thompson and Wallace, 1998).

SST anomalies coherently varying with the AO (Fig. 5b) are observed both in the North Atlantic and the North Pacific. Positive anomalies are found in the western and central North Pacific and from the eastern United States to the western Europe. The sea south of Greenland takes negative anomalies. There is no significant response in the tropical Pacific of both atmospheric and SST anomaly fields, while the equatorial Atlantic has a negative response.

The regression map of SSW anomalies over the North Pacific (Fig. 5c) shows the weakening of wintertime East-Asian monsoon around Japan and the anticyclonic wind circulation with easterly wind anomalies along the zonal band of 20–50°N over the North Pacific. The latter corresponds to the weakening of the AL as shown in Fig. 5e.

The regions, which have a strong pressure gradient anomaly associated with a strong wind anomaly, are consistent with the SST response regions in the North Atlantic

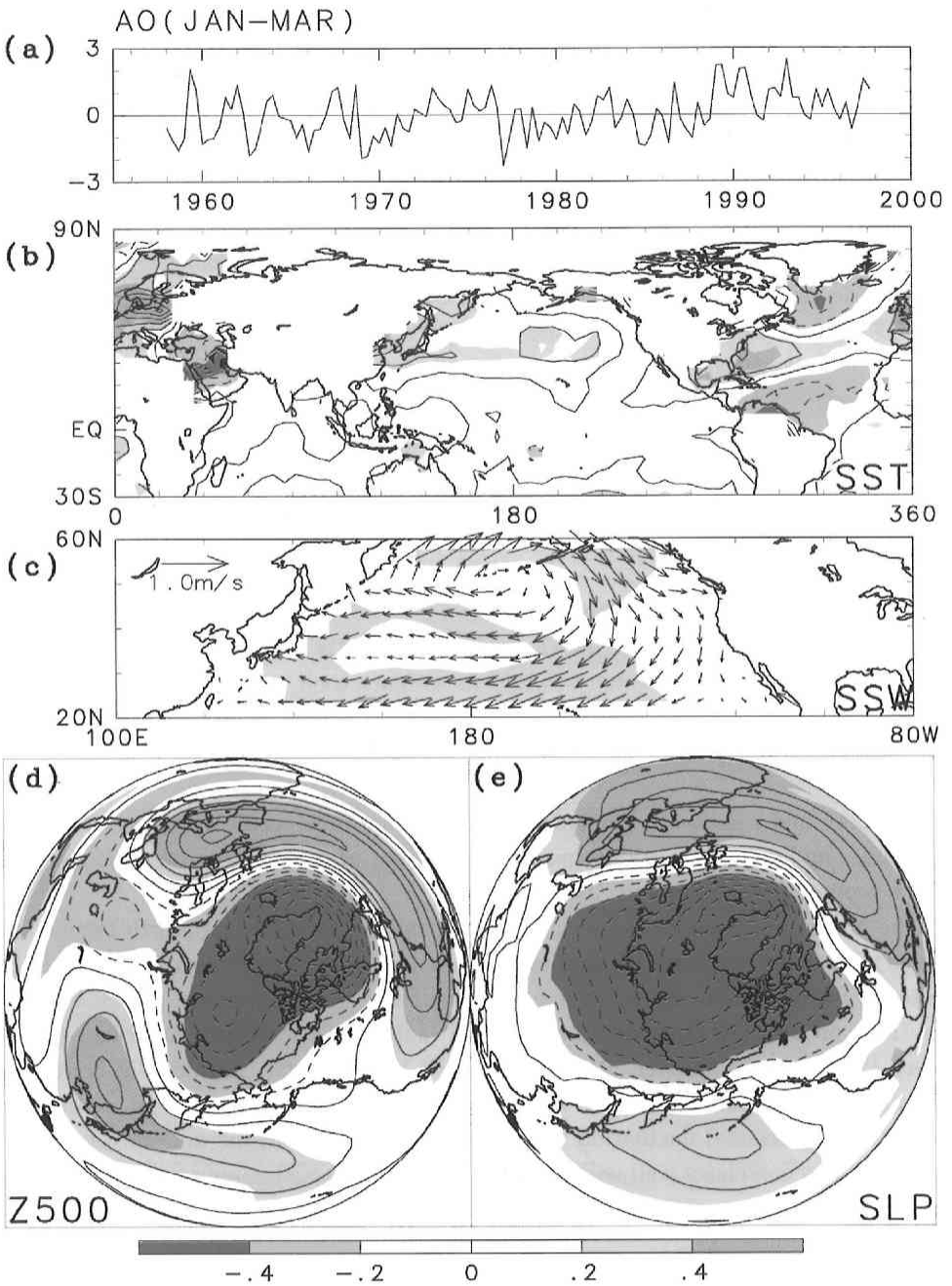

Fig. 5. (a) Standardized winter (January through March) AO index given by Thompson and Wallace (2000). Anomalies of (b) SST, (c) SSW, (d) 500 hPa geopotential height and (e) SLP, which are regressed upon the standardized AO index shown in (a). Contour intervals in (b), (d) and (e) are 0.1 K, 10 m and 1 hPa, respectively. Shadings are given based on correlation coefficients with the AO index. Negative contours are dashed.

and the North Pacific.

In the North Pacific sector, the weaker wintertime East-Asian monsoon and the AL can cause a smaller amount of the heat release from the ocean and a less equatorward cold water advection by Ekman transport in the western North Pacific (Yasuda and Hanawa, 1999). Therefore, positive SST anomalies in the western midlatitudes should result from both less heat loss through the surface and weaker Ekman transport of cold water in this region.

In the North Atlantic sector, a relationship between SST anomalies and anomalous atmospheric circulation is the same as that of the NAO. As pointed out in Walker and Bliss (1932), a stronger IL should cause enhanced cold water advection and heat release over the Greenland-Labrador Sea and enhanced southwesterly winds of mild marine air over the northwestern Europe. The corresponding positive SLP anomalies at lower latitudes over the Atlantic Ocean and the Mediterranean; that is, the stronger AH should be accompanied by warm southeasterly winds to the southeastern United States. Northeasterly winds corresponding to the stronger AH might be responsible for the appearance of negative anomalies in the equatorial Atlantic.

4.2. EOF analyses for SST anomaly fields

In this subsection, changing the viewpoint, we directly detect organized patterns of SST anomaly fields by EOF analysis, and investigate their relationship with the AO. Using all months of the year, EOF analysis are performed by a covariance matrix method to the monthly mean SST anomalies in the region north of 20°N from 1958 to 1997.

Figures 6 and 7 show the standardized wintertime time coefficients of the first two EOF modes and distributions of regression coefficient of the monthly mean SST, SSW, 500hPa geopotential height and SLP anomalies.

The first mode in SST fields (Fig. 6b) has a signal in the central North Pacific and a signal with the reversed sign along the west coast of North America extending over the equatorial Pacific. The regression maps of 500 hPa geopotential height and SLP anomalies (Figs. 6d and 6e) represent the reversed (anti-) Pacific/North American (PNA) pattern (Wallace and Gutzler, 1981). The SSW in the North Pacific (Fig. 6c) shows anticyclonic feature corresponding with the weaker AL. Time coefficient of the first mode reveals a decadal fluctuation with the jumps occurred in the mid-1970's and the late-1980's, and correlates well with the PNA index ($R=-0.55$; January). This finding is consistent with the other studies (*e.g.*, Nitta and Yamada, 1989; Trenberth, 1990; Tanimoto *et al.*, 1993, 1997).

As shown in Fig. 7, the mode closely relating to the AO appears as the second mode. Actually, the correlation coefficient between the AO index and time coefficient of the second mode is 0.51 in winter, which exceeds the 95% significant level by the student t-test. This mode has a strong signal in the midlatitudes of the North Pacific and the North Atlantic with one polarity and a weak response in the sea south of Greenland with another polarity. The regression maps of 500 hPa geopotential height and SLP anom-

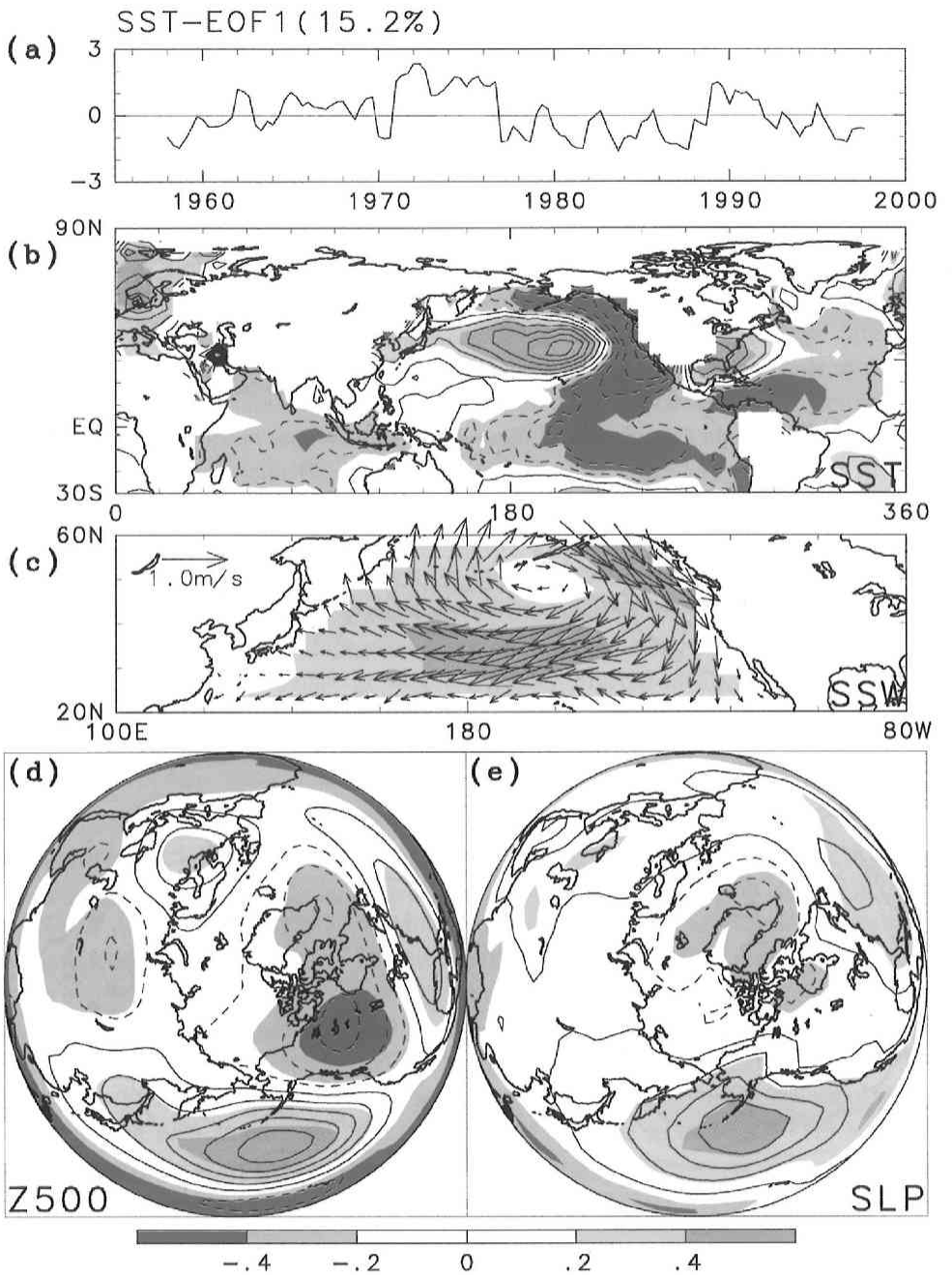

Fig. 6. (a) Standardized winter (January through March) time coefficient of the first SST-EOF mode, obtained in the regions north of 20°N from 1958 to 1997 using all months of the year, and anomalies of (b) SST, (c) SSW, (d) 500 hPa geopotential height and (e) SLP, which are regressed upon the standardized time coefficient shown in (a). Contour intervals in (b), (d) and (e) are 0.1 K, 10 m and 1 hPa, respectively. Shadings are given based on correlation coefficients with the time coefficient. Negative contours are dashed.

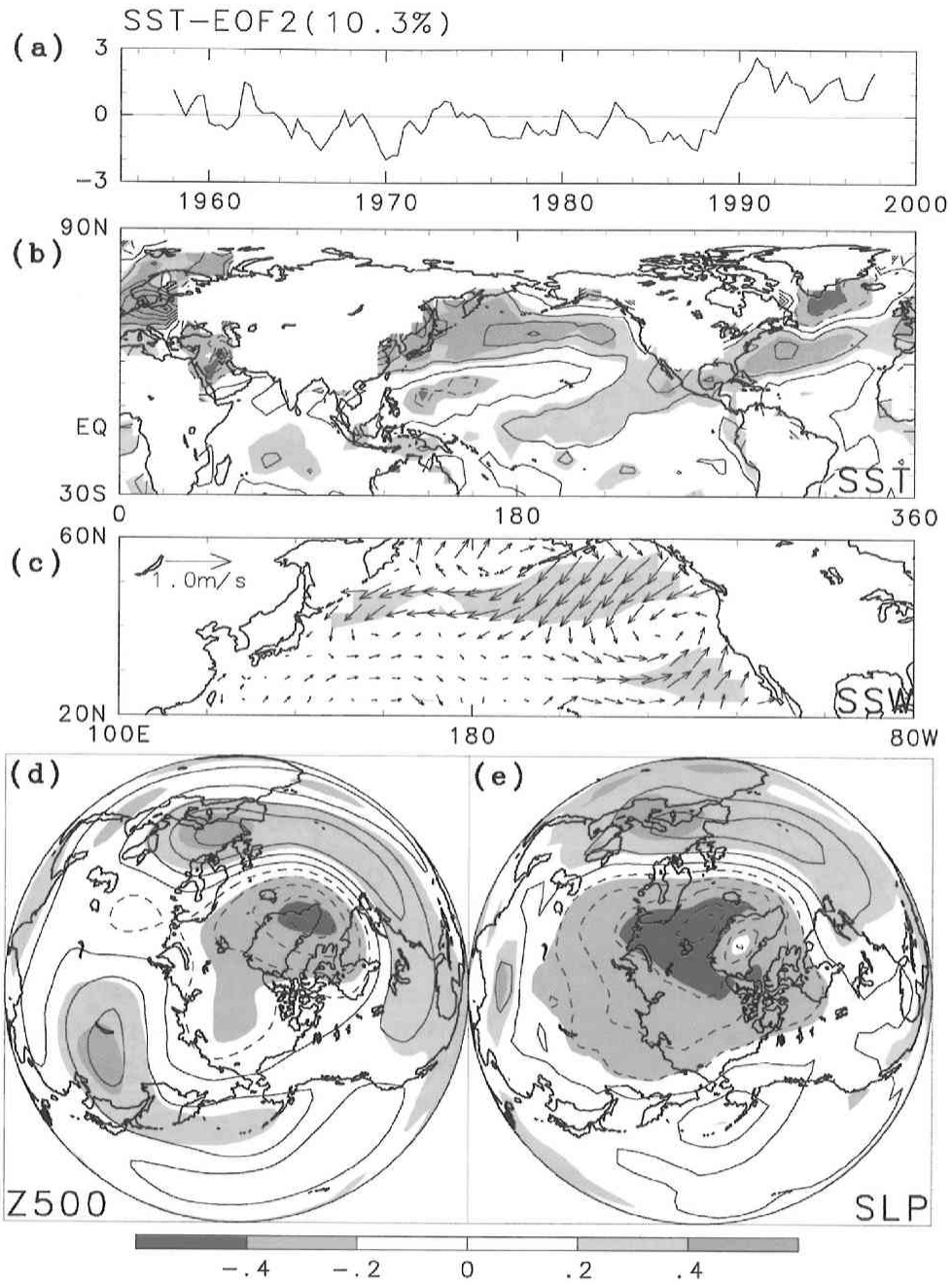

Fig. 7. Same as Fig. 6 except for the second mode.

alies (Figs. 7d and 7e) are very similar to the regression upon the AO index (Fig. 5). They show a strong signal in the polar region and a weak signal with opposite sign in the North Atlantic. In the North Pacific, the AL response in the atmospheric fields is not

as clear as that of the AO. The reason why magnitudes of the signals are bigger in the SST field and smaller in the atmospheric fields than that of the regression maps of the AO is that the former represents a leading mode in the SST field while the later does in the SLP field.

4.3. Climate jump in the late-1980's

Much attention has recently been devoted to variability in the North Pacific on decadal time scale. This variability is found in SST, SLP, and biological productivity as well as the other variables (*e.g.*, Tanimoto *et al.*, 1993). In these fluctuations, several climate jumps have been pointed out in the 1940's, the mid-1970's and the late-1980's (Nitta and Yamada, 1989; Zhang *et al.*, 1997). The cause and mechanisms of the low-frequency climate variability in the North Pacific have not been fully understood yet.

Although Thompson and Wallace (1998) pointed out the AO index exhibited a trend toward the high index polarity over the past few decades, it can be said that the AO index has an abrupt change in 1988/89 (see Fig. 5a). This jump is also seen in time coefficient of the second SST-EOF mode shown in Fig. 7a. A change in winter mean standardized AO index between the two periods of 1980-88 and 1989-97 is 1.64 and this jump exceeds the 95% significant level. It corresponds to the 9.5 hPa decreasing of SLP over the North Pole region and the 3 hPa weakening of the AL.

Figure 8 shows the change in winter (January-March) mean SST, SSW, 500 hPa geopotantial height and SLP anomalies between the two periods of 1980-88 and 1989-97. These are similar in shape to the regression maps on the AO (Fig. 5) and the second SST-EOF mode (Fig. 7). The jumps in the atmospheric fields are characterized by the minimum at the pole surrounded by a zonal ring of opposite sign, and it is zonally symmetric, that is, the stronger polar jet, the stronger IL and the weaker AL. The change of the SST field has a positive signal in the midlatitudes of the North Pacific and the North Atlantic and a negative signal in the sea south of Greenland. However the change of variables in the North Pacific is a little stronger than the regression of the AO or the second SST-EOF mode. It is found that the first SST-EOF mode also has a jump in the late-1980's, though it is smaller than that of the AO or the second SST-EOF mode. Maps averaging the first and second SST-EOF regression maps weighted by their jump magnitude (EOF1 : EOF2 = 0.82 : 1.97 ; Fig. 9) are identical to the difference maps (Fig. 8). Therefore the 1988/89 climate jump is associated with the second SST-EOF mode (*i.e.*, AO) and partially with the first SST-EOF mode (*i.e.*, PNA).

On the other hand, well-known climate jump in 1976/77 appears only in the first SST-EOF mode (see Fig. 6a). The changes between the two periods of 1967-76 and 1977-86 (not shown here) are quite similar feature to the regression maps of the first SST-EOF mode (Fig. 6) in the whole area. That is, the 1976/77 climate jump is associated with the jump of the PNA activities.

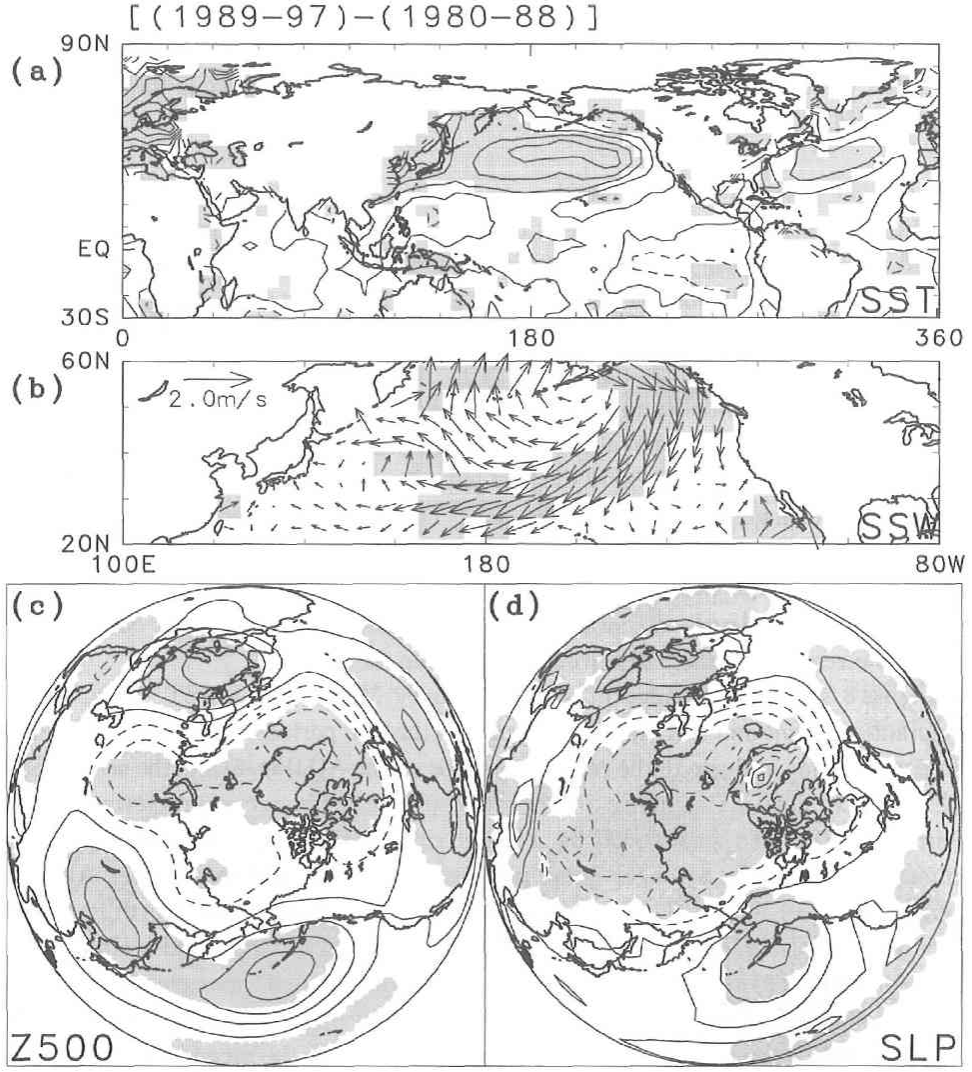

Fig. 8. Changes in winter (January-March) mean anomalies of (a) SST, (b) SSW, (c) 500 hPa geopotential height and (d) SLP between the two periods of 1980-88 (low index period) and 1989-97 (high). Contour intervals in (a), (c) and (d) are 0.2 K, 20 m and 2 hPa, respectively. Negative contours are dashed. Dotted regions are those in which the difference exceeds the 95% significance level.

5. Summary

In the present study, EOF and REOF analyses were applied to the monthly mean SLP anomalies for the region north of 20°N to investigate the relationship between the AO and the NAO or the POL. To examine SST anomaly fields coherently varying with the AO, regression analyses were performed. In addition, EOF analysis was applied to monthly mean SST fields to examine the climate jump that occurred in the late-1980's

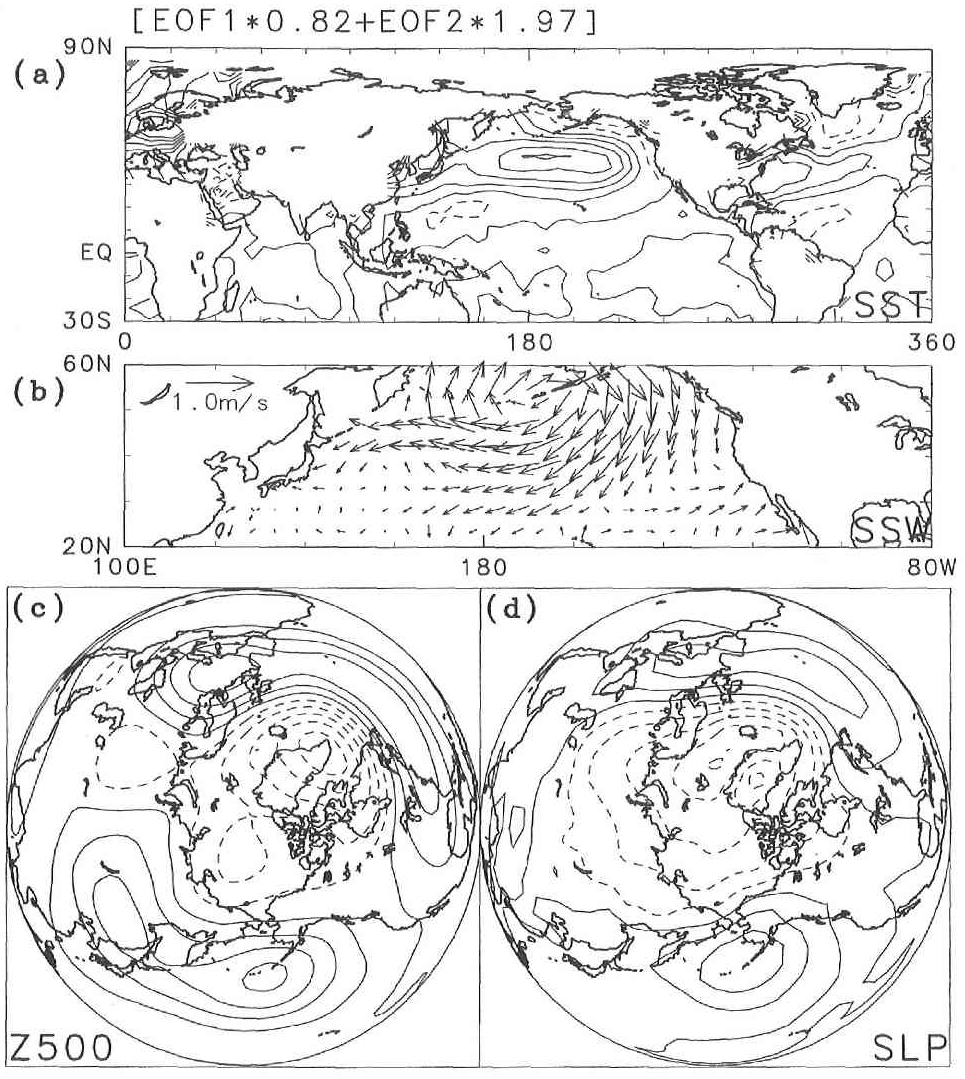

Fig. 9. Reconstructed maps using the first and second SST-EOF regression maps of (a) SST, (b) SSW, (c) 500 hPa geopotential height and (d) SLP anomalies, which are summed with weights according to their magnitudes in 1988/89 climate jump. Contour intervals in (a), (c) and (d) are 0.2 K, 20 m and 2 hPa, respectively. Negative contours are dashed.

and to clarify its relationship with the AO. Main results can be summarized as follows:

1. The AO is the dominant mode over the Northern Hemisphere SLP fields and includes the variabilities designated as the NAO and the POL.

2. SST anomaly fields coherently varying with the AO were found in the North Atlantic and the North Pacific. The regression maps of SLP and 500 hPa geopotential height anomalies upon the AO index showed that the AO includes activities of both the

IL and the AL. The regression map of SSW anomalies showed the variabilities of wintertime East-Asian monsoon and anomalous anticyclonic circulation over the North Pacific.

3. The first SST-EOF mode revealed the decadal fluctuation with the jump occurring in the mid-1970's and the late-1980's, and it was found that this mode is associated with the PNA. The mode coherently varying with the AO appeared as the second mode.

4. The AO index showed the significant jump in 1988/89. This 1988/89 climate jump was also found in SST and atmospheric fields, and could be described by the second SST-EOF mode (*i.e.*, AO) and partially in the first SST-EOF mode (*i.e.*, PNA). On the other hand, the well-known climate jump occurring in 1976/77 appeared only in the first SST-EOF mode.

It was revealed that the AO is the dominant made not only in the SLP field but also in the SST field. Variabilities of the wintertime polar vortex occur with the AO from sea level to the lower stratosphere (Thompson and Wallace, 1998 ; 2000). The direction of cause and effect between the atmosphere and the ocean is not understood by the result of this study. More investigation is needed to reveal a mechanism of the AO.

Many recent studies suggest that the low frequency climate variability in the North Pacific is caused by tropical forcing (*e.g.*, Nitta and Yamada, 1989 ; Graham 1994), while several studies suggest that the air-sea coupled system in the extratropical North Pacific may cause interdecadal variability by itself (Latif and Barnett, 1996). The present study reveals that there are various types of climate jumps in the system. So, several mechanisms might exist. More investigation on decadal climate variability including abrupt changes may be very interesting subject and should be done in near feature.

Acknowledgment : The authors thank Dr. H. Nakamura for providing useful comments. Kengo Miyamoto kindly provided the SLP data. Thanks are also extended to members of the Physical Oceanography Laboratory at Tohoku University for their useful comments and heartfelt encouragement.

References

Barnston, A.G. and R.E. Livezey, 1987 : Classification, seasonality and persistence of low-frequency atmospheric circulation pattern, *Mon. Wea. Rev.*, **115**, 1083-1126.

Bell, G.D. and M.S. Halpert, 1995 : Atlas of intraseasonal and interannual variability, 1986-1993, *NOAA Atlas No. 12*, Climate Prediction Center, NOAA/NWS/MNC. Washington, DC.

Deser, C., 2000 : On the teleconnectivity of the "Arctic Oscillation", *Geophys. Res. Lett.*, **27**, 779-782.

Graham, N.E., 1994 : Decadal-scale climate variability in the 1970s and 1980s : Observations and model results, *Climate Dyn.*, **10**, 135-162.

Hanawa, K. and T. Yasuda, 2000 : Reconstruction of sea surface wind fields over the North Pacific using sea level pressure fields during the period of 1899-1995, *J. Meteor. Soc. Japan*, **78**, 731-751.

Horel, J.D., 1981 : A rotated principal component analysis of the inter annual variability of the Northern Hemisphere 500 mb Height field, *Mon. Wea. Rev.*, **109**, 2080-2092.

Kachi, M. and T. Nitta, 1997 : Decadal variations of the global atmosphere-ocean system, *J. Meteor. Soc. Japan*, **75**, 657-675.

Kalnay, E.M. and Coauthors, 1996: The NCEP/NCAR reanalysis project, *Bull. Amer. Meteor. Soc.*, **77**, 437-471.

Kerr, R.A., 1998: A new force in high-latitude climate, *Science*, **284**, 241-242.

Latif, M. and T.P. Barnett, 1996: Decadal climate variability over the North Pacific and North America: Dynamics and predictability, *J. Clim.*, **9**, 2407-2423.

Manabe, T., 1999: The digitized Kobe Collection: Historical surface marine meteorological observations in the archival of the Japan Meteorological Agency, *Bull. Amer. Meteor. Soc.*, **80**, 2703-2715.

Miyamoto, K., 2000: Reconstruction of sea surface wind and wind stress fields in the Northern Hemisphere during the last centenary. Doctoral Thesis, Tohoku Univ., 137 pp.

Nitta, T. and S. Yamada, 1989: Recent warming of tropical sea surface temperature and its relationship to the Northern Hemisphere circulation, *J. Meteor. Soc. Japan*, **67**, 375-383.

Overland, J.E., J.M. Adams and N.A. Boud, 1999: Decadal variability of the Aleutian Low and its relation to high-latitude circulation, *J. Clim.*, **12**, 1542-1548.

Preisendorfer, R.W, 1988: Diagnostic procedure via PCA and FA, *Principal component analysis in meteorology and oceanography*, ELSEVIER, 265-292.

Richman, M.B., 1986: Rotation of principal components, *J. Clim.*, **6**, 293-335.

Tachibana, Y., M. Honda and K. Takeuchi, 1996: The abrupt decrease of the sea ice over the southern part of the Sea of Okhotsk in 1989 and its relation to the recent weakening of the Aleutian Low, *J. Meteor. Soc. Japan*, **74**, 579-584.

Tanimoto, Y., N. Iwasaka, K. Hanawa and Y. Toba, 1993: Characteristic variations of sea surface temperature with multiple time scales in the North Pacific, *J. Clim.*, **6**, 1153-1160.

Tanimoto, Y., N. Iwasaka and K. Hanawa, 1997: Relationship between sea surface temperature, the atmospheric circulation and air-sea fluxes on multiple time scales, *J. Meteor. Soc. Japan*, **75**, 831-849.

Thompson, D.J.W. and J.M. Wallace, 1998: The Arctic Oscillation signature in wintertime geopotential height and temperature field, *Geophys. Res. Lett.*, **25**, 1297-1300.

Thompson, D.J.W. and J.M. Wallace, 2000: Annular modes in the extratropical circulation. Part I: Month-to-month variability, *J. Clim.*, **13**, 1000-1017.

Thompson, D.J.W., J.M. Wallace and G.C. Hegerl, 2000: Annular modes in the extratropical circulation. Part II: Trend, *J. Clim.*, **13**, 1018-1036.

Trenberth, K.E., 1990: Recent observed interdecadal climate changes in the Northern Hemisphere, *Bull. Amer. Meteor. Soc.*, **71**, 988-993.

Trenberth, K.E. and D.A. Paolino, 1980: The Northern Hemisphere sea level pressure dataset, *Mon. Wea. Rev.*, **108**, 855-872.

Waker, G.T. and E.W. Bliss, 1932: World Weather V, *Mem. Roy. Meteor. Soc.*, **4**, 53-84.

Wallace, J.M. and D.S. Gutzler, 1981: Teleconnections in the geopotential height field during the Northern Hemisphere winter, *Mon. Wea. Rev.*, **109**, 784-812.

Wallace, J.M., 2000: North Atlantic Oscillation/annular mode: Two paradigms-one phenomenon, *Q. J. R. Meteorol. Soc.*, **126**, 791-805.

Walsh, J.E., W.L. Chapman and T.L. Shy, 1996: Recent decrease of sea level pressure in the central Arctic, *J. Clim.*, **9**, 480-486.

Wang, J. and M. Ikeda, 2000: Arctic Oscillation and Arctic Sea-Ice Oscillation, *Geophys. Res. Lett.*, **27**, 1287-1290.

Ward, M.N., 1989: On the estimation of EOF time coefficients when data are missing, *Meteorological Office Synoptic Climatology Branch Discussion Note 114*.

Yasuda, T. and K. Hanawa, 1999: Composite analysis of North Pacific Subtropical Mode Water properties with respect to the strength of the wintertime East Asian monsoon, *J. Oceanogr.*, **55**, 531-541.

Zhang, Y., J.M. Wallace and D.S. Battisti, 1997: ENSO-like interdecadal variability: 1900-93, *J. Clim.*, **10**, 1004-1020.